Morphological and histochemical observations of the organic components of ostrich eggshell

P D G Richards[a*], A Botha[b] and P A Richards[c]

ABSTRACT

The organic component of the avian eggshell can be divided into 3 portions, the shell membranes, the matrix and the cuticle. These have been well characterised in the chicken but little has been published with regard to the ostrich (*Struthio camelus*). A number of recent studies have indicated that the cause of intra-shell embryonic deaths in the ostrich is similar to intra-shell embryonic deaths that occur in the chicken. These deaths in the chicken are associated with the loss of or damage to the waxy cuticle and other organic components of the eggshell, which is reported to be absent in the ostrich eggshell. In this study, preliminary morphological and histochemical analyses, at the level of the light and electron microscope, have characterised the various organic components of the ostrich eggshell. The results of the histochemical and electron microscopical analyses suggest that there may only be 1 shell membrane in this species, which could play a major role in the limitation of bacterial penetration to the embryonic chamber. The shell membrane has a distinct elemental profile as determined by EDS analysis. The matrix is shown to decrease in mesh size from the mammillary layer to the vertical crystal layer. The closer packing of the mesh may indicate the presence of a morphologically discernible termination signal to calcification or the remnants of an evolutionary calcified cuticle. The matrix of the pores may also form a defensive barrier against bacterial invasion, which could be damaged as a result of dipping the eggs before incubation.

Key words: glycoconjugate, histocytochemistry, lectins, ratite, ultrastructure.

Richards P D G, Botha A, Richards P A **Morphological and histochemical observations of the organic components of ostrich eggshell.** *Journal of the South African Veterinary Association* (2002) 73(1): 13–22 (En.). Department of Anatomy, Faculty of Medicine, University of Pretoria, Pretoria, 0001 South Africa.

INTRODUCTION

Most avian eggshells have 3 distinct organic components interwoven into the structure of the shell. These are the shell membranes (inner (ISM) and outer (OSM)), shell matrix and shell accessory material or cuticle. The egg of the domestic hen, being the most readily available, has been extensively studied with regard to the morphology and histochemistry of its organic components. These components have been determined using both immunohistochemical and biochemical techniques[2]. Although all 3 layers contain glycoconjugates, namely proteoglycans and glycoproteins, each layer differs in its composition and structure[1].

The shell membranes of the chicken egg are clearly distinguishable from each other, where the ISM is generally thinner than the OSM and consists of smaller fibres in a more compact weave[6,36]. The fibres themselves consist of a collagenous protein core (Type I in the OSM and Type V in the ISM, with Type X being found throughout) and a mucopolysaccharide mantle (sulphated glycoproteins, in particular keratan sulphate in the OSM)[2]. In the chicken there is an intact limiting membrane at the junction between the shell membranes and the chorio-allantoic membrane (CAM) that appears to be constructed from the mantle material covering the individual fibres[6]. Little is known about the function of the 2 shell membranes except that the outer surface of the OSM is important in the determination of the calcification of the shell[2]. While the barrier properties of the membranes to bacteria are limited[16]. It has been proposed that it is the architecture of the shell as a whole that limits bacterial invasion[22]. In a previous study, the relationship of the OSM to the mammillary layer and to the calcification of the eggshell in the ostrich (*Struthio camelus australis* var. *domesticus*) was described[29], postulating the presence of type X collagen in cup-shaped structures on the calcification surface. No other detailed study, however, has been undertaken on these components of the ostrich eggshell.

The shell matrix is the major organic component of the shell, being predominantly composed of polysaccharides (11 %) and proteins (70 %)[4], with most of the amino acid residues being either glutamic or aspartic acid[2]. Calcified tissue such as bone, teeth, and molluscan shells have a proportion of γ-carboxy glutamic acid residues[19] that are also present in the matrix of the domestic hen's egg as ovocalcin, a calcium-binding protein[2]. Keratan sulphate and dermatan sulphate have been shown to be the main proteoglycans present in the matrix[1]. The function of the shell matrix is probably that of a foundation for the calcification process, where eggshell calcification may follow the Garcia-Ruiz model, with the organic matrix acting as the membrane, which in turn controls the calcification process[14].

The shell accessory material or cuticle of the eggshell is located on the outer surface of the shell and is found in most avian species. If present, it is organised in 1 of 4 basic forms: plugged[8], chalky crystalline[37], organic spherical[4] and organic featureless[9]. The organic cuticle varies in thickness from 0.5 mm to 12.8 mm and is composed of glycoconjugates whose precise composition is unknown[2,15]. The glycoconjugates of this layer are associated with high molecular weight glycoproteins that have many disulphide and free sulphhydryl groups[2]. In the domestic hen the cuticle performs 2 functions with regard to the egg and its contents. Its primary function is the control of water loss and gaseous exchange. In this instance the cuticle's permeability to water and conductance of gases is dependent on the relative humidity of the surrounding environment[25]. The layer's secondary function is as a protective barrier against microbial invasion. The protective process may be similar to the mechanism whereby glycoconjugates work in the inner ear and reproductive tract of mammals[7,13]. In the inner ear the glycoconjugates have specific antibodies against the bacterial surface proteins[7],

[a]Department of Anatomy, Faculty of Medicine, University of Pretoria, Pretoria, 0001 South Africa.

[b]Microscopy and Microanalysis Unit, University of Pretoria, Pretoria, 0002 South Africa.

[c]eFACT Consultancy (Pty) Ltd., 856 30th Avenue, Villieria, Pretoria, 0186 South Africa.

*Author for correspondence. 856 30th Avenue, Villieria, Pretoria, 0186 South Africa.
E-mail: grichards@mweb.co.za

Received: May 2001. Accepted: January 2002.

and similar antibodies may also be present in the cuticle's glycoconjugates. Alternatively the cuticle may contain glycoconjugates similar to Muc 1/ episialin, which act as effective barrier glycoconjugates in mammalian uteri[13].

In the ostrich only the deeper organic structures, namely the membranes and matrix, are reported to be present[35]. Despite earlier histological reports of this species' eggshell[20,38] indicating a possible basis for persistent anecdotal reports of a cuticle[35], it is generally accepted that these shells do not possess an organic cuticle[18]. However, intra-shell embryonic death and low hatchability in the ostrich have been linked to the failure of the 2 roles that the cuticle performs[10,18]. The authors of a recent study have postulated the presence of a calcified organic layer on the outer surface of these eggshells, based on energy dispersive X-ray analysis investigations[29]. The present uncertainty about the role of similar organic components in the ostrich suggests that a greater understanding of these organic components of the shell is required. Such an increase in knowledge may lead to changes in handling, incubation and diet in order to obtain better hatchability and survival rates in commercial ostrich farming. This study examines the main organic components of the ostrich eggshell, namely the matrix and the shell membranes, as part of a comprehensive investigation into the structure of the ostrich eggshell.

MATERIALS AND METHODS

Ostrich eggshells were obtained from farms in the vicinity of Onderstepoort, Gauteng, South Africa. All eggshells were from fertile eggs that had not been associated with incubation or hatching problems. The eggs had not been dipped in chemical solution to clean them, before incubation, but rather had been wiped clean.

Shell membrane (SM) that had dried and peeled from the inner surface of the shell was cut into specimens of approximately 10 mm^2 before being processed for light microscopy (LM), transmission electron microscopy (TEM), scanning electron microscopy (SEM) and EDS. Pieces of eggshell (approximately 10 × 20 mm) were also removed from the collected eggshells. These specimens were deep-etched in a solution of 8 % ethylenediaminetetracetic acid (EDTA) and 6 % formaldehyde for a period of not less than 48 days, following which a gelatinous layer was removed from the outer surface of the deep-etched shell specimens. The gelatinous material was processed for LM, TEM, SEM and EDS. Deep-etched shell fragments retaining the gelatinous material were also processed for SEM and EDS. In order to obtain fully decalcified samples of ostrich eggshell, samples from the eggshells were vacuum embedded in resin, and 10 µm radial cross-sections, through the calcified shell, were obtained using a sledge microtome. These sections were decalcified with 8 % EDTA and 6 % formaldehyde over a period of 48 hours. The resulting translucent sections were processed for LM, TEM and, following EDS analysis, for SEM.

The specimens for LM were processed to wax using standard techniques. Five micrometre wax sections were cut and picked up on silanated slides[26]. The sections were dewaxed and stained with haematoxylin and eosin, Masson's trichrome, periodic acid Schiff's reagent, high-iron diamine and alcian blue at various pHs (0.2–3.2), all using standard protocols[5]. To determine the presence of sialadase-resistant glycoconjugates, sections of membrane were incubated with the sialidase enzyme before being stained with alcian blue[5]. Furthermore, de-waxed sections were stained with 3 lectins (peanut, con-conavalin A (Con A) and wheat germ) (Sigma, USA) using a standard lectin histochemical procedure[12]. In addition, sections of shell membrane were treated using the high temperature methylation-saponification technique of Spicer and Lillie[5]. Measurements of the size of the various components were obtained using a calibrated inter-ocular micrometer. Ten measurements were taken from each layer in 10 separate shell membrane sections.

The samples processed for TEM were fixed in 2.5 % glutaraldehyde in phosphate buffer (pH 7.2) for 60 minutes. They were then postfixed in phosphate buffered osmium tetroxide (pH 7.2) for 30 minutes at room temperature. The samples were dehydrated in an ascending alcohol series and embedded in LR White® resin. Thin sections were obtained using a Reichart Ultracut® ultramicrotome and stained with uranyl acetate and lead citrate before being examined using a Philips® 301 at an accelerating voltage of 80 kV. The measurements from the TEM were obtained from 5 randomly taken micrographs from 5 specimens. At least 10 measurements were taken from selected features within each micrograph.

The SEM samples were either viewed as dry samples or fixed as for TEM. The fixed samples were dehydrated in an ascending alcohol series and critical-point dried. All the SEM samples were mounted on aluminium stubs and gold sputter-coated. The coated samples were examined using a JEOL® 840 scanning electron microscope at an accelerating voltage of 5 kV. Micrographs from 5 randomly selected areas of 3 membrane preparations were used for the measurement of the membrane and its fibres. At least 10 measurements of membrane width and fibre size were made in each of the random areas.

The EDS samples were fixed in 2.5 % glutaraldehyde as for the TEM and SEM specimens but were not osmicated. The EDS samples were then dehydrated in the same manner as the SEM samples before being mounted on brass stubs using silver paint to avoid peak overlap during the analysis. The samples were not sputter-coated before being analysed in low vacuum conditions (0.3 torr) using a Noran Voyager® EDS system attached to a JEOL® 5800LV microscope operated at an accelerating voltage of 25 kV. The shell membrane specimens were measured and 10 equidistant areas (probe sites) were analysed across 3 membrane samples from the CAM interface (probe site 1) to the mammillary layer interface (probe site 10) (Fig. 1a). Ten randomly paired areas on the 5 shell fragments that had retained the gelatinous material following EDTA treatment and 10 randomly selected areas of a separate specimen of gelatinous material were analysed by EDS. The paired areas corresponded, as far as possible, to the 2 areas that had been analysed in a previous study using calcified eggshells[27]. Area A was within the gelatinous material on the external surface of the eggshell while area B was deep to this in the partially deep-etched shell (Fig. 1c, d).

The de-calcified 10 µm cross-sections of eggshell that were analysed using the SEM were processed and mounted as for EDS analysis. The EDS analysis of these specimens was used as a confirmatory process to ensure that the specimens being examined did not show a calcium peak, thus confirming the absence of calcium ions in these sections, an indication that full decalcification had been obtained using the decalcification process outlined above. Following EDS analysis the sectioned material was gold sputter-coated and viewed using the JEOL® 840 as outlined above.

RESULTS

Light microscopy

Shell membrane

Examination of the haemotoxylin and eosin-stained sections of the SM clearly revealed a nucleus-free fibrous tissue. Three distinct layers could be distinguished. Layer I, the thinnest of the 3 layers, lay closest to and appeared to be

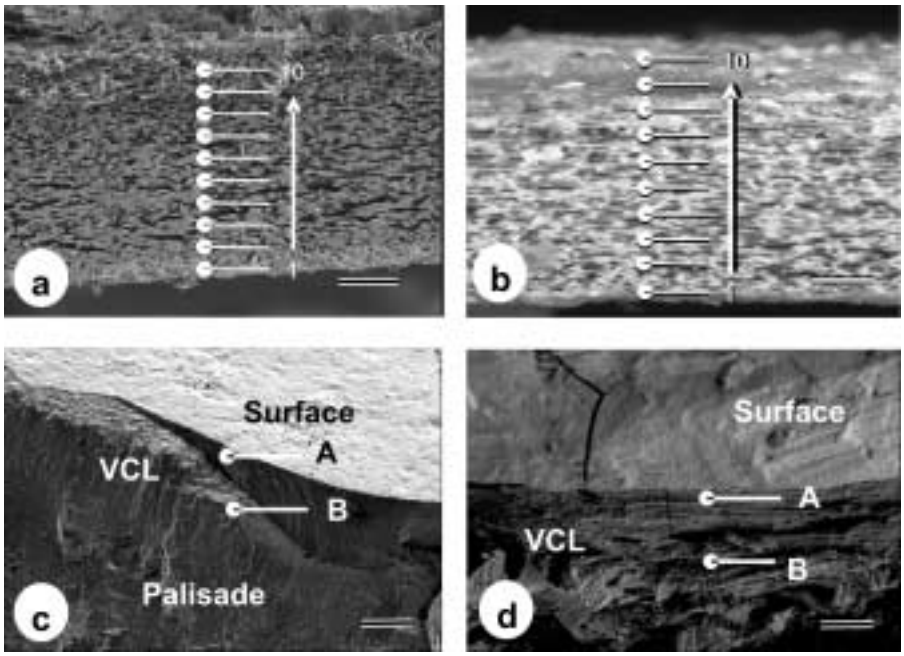

Fig. 1: **Scanning electron micrographs of** (a) **sputter-coated shell membrane and** (b) **uncoated shell membrane** (positions 1–10 marked) **– both samples orientated to show the calcification surface/mammillary layer interface towards the top of the micrograph;** (c) **calcified and** (d) **deep-etched shells orientated with the outer surface towards the top. ●— = approximate positions of the EDS probe sites; VCL = vertical crystal layer.** (Scale bars: a, 50 µm; b,10 µm; c, d, 20 µm.)

closely associated with the CAM (Fig. 2a). The middle layer, layer II, was the thickest and had an open, loose weave, while the outer layer, layer III, had a more compact weave (Fig. 2a). The average diameter of the measured fibres within each layer (layer I = 2.3 ± 0.9, layer II = 3.0 ± 1.0, layer III = 3.0 ± 1.0) showed large intra-layer variation. The intra-layer variation meant that inter-layer measurements showed no significant statistical difference using a Student's *t*-test. Therefore the average diameter of the fibres from the membrane as a complete unit, when measured at the light microscopy level is shown in Table 1. Cup-shaped structures were present on the calcification surface, i.e. the surface of the SM that would be in contact with the mammillary layer of the calcified shell. These were intimately linked to the outer fibres of layer III of the SM. All 3 layers of the SM stained distinctly red with the Masson's trichrome stain except for the cup-shaped structures on the calcification surface, which stained blue/green.

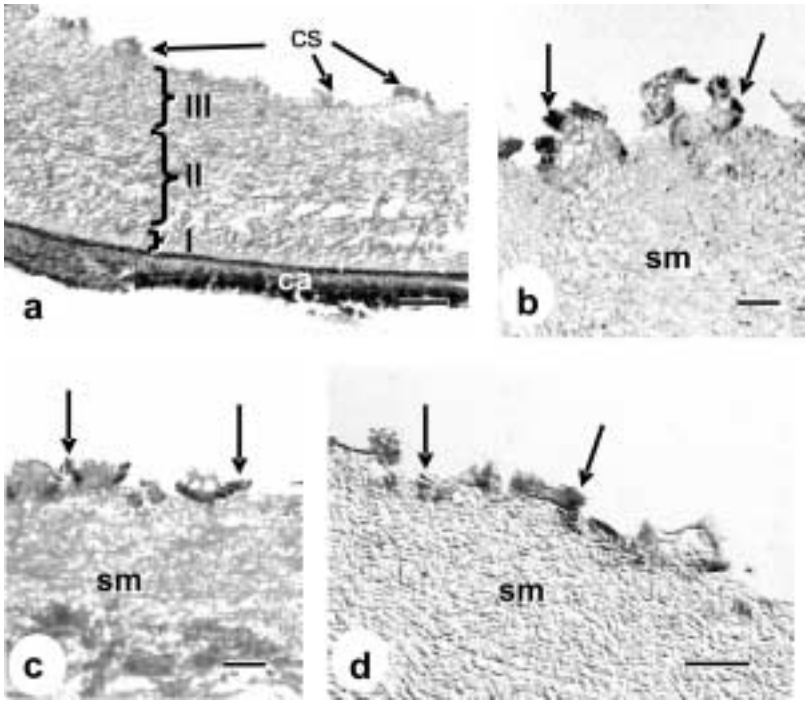

Fig. 2: **Light micrographs of sections of ostrich shell membrane;** a: **haematoxylin and eosin-stained section – the 3 layers** (layers I–III) **are bracketed, ca = chorio-allantoic membrane, cs = calcification surface;** b: **alcian blue-** (pH = 3.2) **stained section;** c: **methylation–saponification treatment of the shell membrane;** d: **differential interference contrast image of a peanut lectin-stained section of shell membrane** (sm)**. Note prominent staining of the cup-shaped structures** (arrows) **on the calcification surface.** (Scale bars: a, 100 µm; b–d 10 µm.)

Both periodic acid Schiff and high-iron diamine staining of the SM proved positive. Qualitative assessment of the alcian blue staining of the membrane demonstrated some differences at the various pH values used (Table 2). The shell membrane stained positive at all the different pH values of alcian blue used, except for that of the lowest (pH = 0.2). However, the calcification surface and the cupped structures were positive at all pH values but were qualitatively more positive than the rest of the SM (Fig. 2b). Although sialidase treatment decreased the level of alcian blue staining of the fibres in all the layers of the SM, there was no decrease in alcian blue staining at the calcification surface. A similar result was obtained with the methylation-saponification stain, where this technique abolished staining of the fibres while retaining the staining of the cup-like structures (Fig. 2c).

Qualitative assessment of the limited lectin histochemistry of the membrane showed that the membrane was positive for both peanut and wheat germ lectin but negative for Con A lectin (Table 3). The calcification surface of the SM demonstrated an increased positivity for both of these lectins (Table 3; Fig. 2d).

Matrix

The matrix underlies the whole of the calcified portion of the shell. Thus, the names of the various regions of the calcified egg[29] were used to orientate the reader when discussing regional variations. Therefore the region closest to the SM was designated the mammillary layer, the mid-region, the palisade layer, and the most exterior region the vertical crystal layer (VCL). The division of the matrix into the 3 regions was undertaken in accordance with previously established criteria for the calcified eggshell[29,35].

No nuclei were present in the shell matrix, as determined from the sections stained with haemotoxylin and eosin. Furthermore, the matrix stained a faint blue colour with Masson's trichrome. The matrix of the shell was PAS negative while retaining the blue-black positivity of the

Table 1: **Morphometry of the shell membrane using the different microscopy techniques. Figures in brackets represent measurements from fixed membrane samples.**

	Light microscopy *n* = 100		Scanning EM *n* = 150		Transmission EM *n* = 250	
	µm	SD	µm	SD	µm	SD
Membrane width	309	17.4	144 (183.5)	10 (8.59)	–	–
Fibre diameter	2.8*	1.0	0.9 (1.7)	0.4 (0.9)	1.47	0.37

*This figure is the mean for all 3 'layers' and therefore represents an *n* of 300.

Table 2: **Histochemical staining characteristics of the ostrich eggshell organic components.**

	AB	AB	AB	AB	AB	PAS	HID
pH	**0.2**	**0.5**	**1.0**	**2.5**	**3.2**		
Membrane							
Layer I	–	+	+	+	++	+++	+
Layer II	–	+	+	+	++	+++	+
Layer III	–	+	+	+	++	+++	+
CS	+	+++	+++	++	+++	+++	+
Matrix							
Mammillary	–	–	+	+	+	–	+
Palisade	±	–	+	+	+	–	+
VCL	++	–	+	+	+	–	+

AB = alcian blue; PAS = periodic acid Schiff; HID = high-iron diamine; CS = calcification surface; VCL = vertical crystal layer.

high-iron diamine stain. It also demonstrated regional variation in the alcian blue staining pattern (Table 2), where the mammillary layer was not stained at the 2 lowest alcian blue pH values (0.2 and 0.5) but was weakly positive at the remaining pH values. The palisade layer had similar staining properties but distinct columns within the layer, which were positive for the lowest alcian blue pH value used (0.2), were demonstrated. The VCL was more positive at the lowest pH (0.2) than at the other pH values used and followed a similar trend to the other layers of the matrix at these pH values. The lectin staining of the matrix was similar to that of the shell membranes in that the Con A lectin proved to be negative while the peanut and wheatgerm lectins were positive, the latter more so than the former (Table 3). The VCL showed an increased affinity for peanut lectin compared to the rest of the matrix.

Transmission electron microscopy

Shell membrane

The shell membrane, when examined using TEM, was seen to consist of a random array of fibres, which displayed no evidence of the presence of distinct layers. The individual fibres were osmiophilic in character and demonstrated little variation in diameter (Table 1). Each fibre had a darker-staining core (Fig. 3a) that made up over 50 % of the average fibre diameter (0.85 ± 0.21 µm). There was evidence of the entrapment of bacterial entities between the fibres (Fig. 3a inset, 3b), where the outer coat of the bacteria was seen to have merged with the outer 'mantle' of the fibres. A limiting membrane (0.09 µm thick, *n* = 30) was observed at the border between the CAM and the shell membrane. The nearest fibres of the SM were attached to this limiting membrane (Fig. 3b). The limiting membrane contained a number of pores and appeared to be formed from material similar to that of the inner core of the fibres. Cup-shaped structures, with the same osmiophilic characteristic of the fibres of the membrane, were present on the calcification surface. However, they lacked the 'mantle' element and, like the limiting membrane, appeared to be composed of material similar to that of the inner core of the fibres.

Table 3: **Lectin histochemical staining characteristics of ostrich eggshell organic components.**

	Peanut	Con-conavalin A	Wheat germ
Membrane			
Layer I	+	–	+
Layer II	+	–	+
Layer III	+	–	+
CS	+++	–	++
Matrix			
Mammillary	+	–	+++
Palisade	+	–	+++
VCL	+++	–	+++

CS = calcification surface; VCL = vertical crystal layer.

Matrix

In decalcified specimens (sections and gelatinous material – see Materials and Methods) the matrix appeared to consist of a network of osmiophilic fibrillar material. The fibrils were approximately 2 ± 0.5 nm in diameter and were arranged in a mesh-like structure (Fig. 3c). In the gelatinous material the fibril strands were more closely packed, similar to structures observed in the decalcified sections of the matrix. These structures appeared to run vertically through the section from the area of the VCL to the mammillary layer. Scattered at random throughout both specimens were profiles delineated by increased osmiophilia and decreased mesh size (Fig. 3c,d). These profiles appeared to represent randomly-orientated sections through tubular structures embedded within the general matrix. The average internal diameter of these tubular structures was 0.8 ± 0.2 µm while the wall of the tube measured 20 ± 2 nm in thickness. The fibrils of the wall, though

more tightly packed, were within the same diameter range as those of the surrounding matrix.

Scanning electron microscopy

Shell membrane

Cross-sections of the dry shell membrane revealed no recognisable layering of this organic portion of the shell. The membranes examined were approximately 144 ± 10 µm thick and were composed of a complex array of intertwining fibrils (Fig. 4a). Although the first 20 µm of the innermost (CAM) side of the membrane appeared to be more compact, there was no clear division between this region and the rest of the membrane. The individual fibres were approximately 1 µm in diameter (Table 1), but the fusion of multiple fibres often made it impossible to determine individual fibre diameters (Fig. 4b). The fibres were arranged in a series of planes, each plane varying between 4 and 6 µm deep, which intertwined in a cross-weave pattern. The individual fibres ran in random directions within the confines of the individual planes. Cup-shaped structures were observed on the calcification surface of the SM. The exposed surfaces of the cup-shaped structures were morphologically similar to the cut surfaces of the fibres (Fig. 4c). No differences were observed in the architectural appearance of the fixed membrane compared to the dry membrane. However, in the fixed specimens the morphology of the fibres suggested the presence of an outer coat covering each fibre (Fig. 4d). The effect of fixation made a significant difference ($P < 0.001$) to the fibre and membrane measurements (Table 1). The individual fibre measurement obtained from the fixed SEM samples was not significantly different from that obtained from the samples prepared for TEM. In the fixed membranes, bacterial particles (cocci) were visible, attached to the outer coat of individual fibres (Fig. 4d inset).

Matrix

In the deep-etched specimens, the mammillary layer could be distinguished by the herringbone pattern of the etched crystallite formations (Fig. 5a). A matrix of fine fibrillar material spanned some of the spaces between each crystallite formation (Fig. 5b). In the palisade layer a more random appearance of the etched crystallites was apparent, while the fibrillar content was in greater evidence (Fig. 5c). No deep-etched crystallites were found in the VCL as the gelatinous material had replaced this region. The outer surface of the gelatinous material resembled the characteristic block structure that is

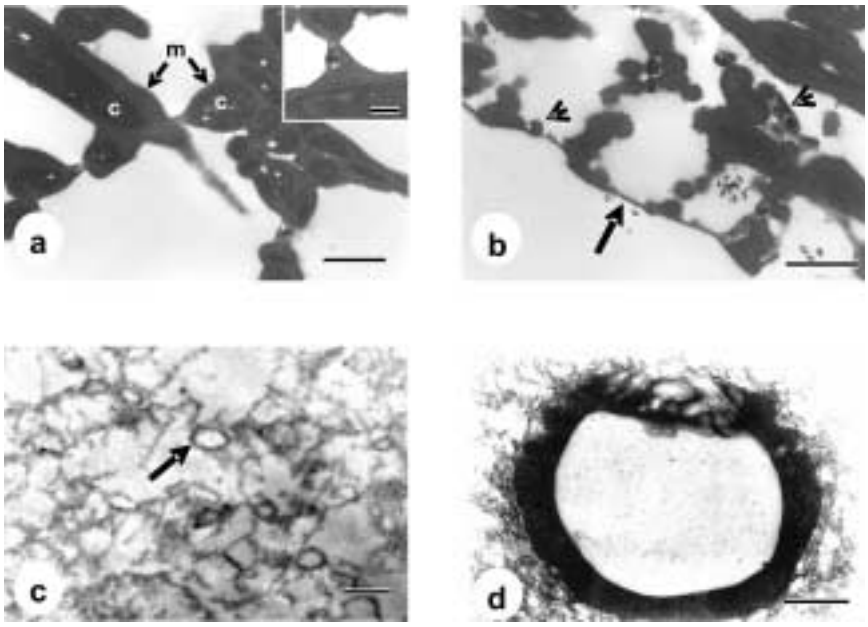

Fig. 3: **Transmission electron micrographs of the shell membrane;** a: **fibres of the shell membrane – note the darker core** (c) **compared to the mantle** (m)**, the inset shows a higher magnification of the entrapment of a bacterial cell;** b: **the limiting membrane** (arrow) **observed at the shell membrane/chorioallantoic membrane interface – note the attachment of fibres to the membrane and the increase in bacterial cells** (arrowheads)**;** c: **low magnification view of the matrix of the ostrich eggshell – note the tubular structures** (arrow) **in the matrix;** d: **increased magnification of the tubular structures in the matrix of ostrich eggshell.** (Scale bars: a, 1 µm; a inset, 0.5 µm; b, 1 µm; c, 1 µm; d, 0.2 µm.)

observed when examining the surface of a calcified eggshell (Fig. 6a). However, in vertical cross-section the material had an amorphous structure with no observable morphological detail (Fig. 6b). The deep-etched specimen contained a number of channels/tubes that appeared to traverse the specimens between the outer and inner surfaces. The course of these channels/tubes was not parallel to the exposed surface and they thus often disappeared into the specimen away from the exposed surface. The channels/tubes were delineated by an unknown material, which appeared to have a fibrous structure, with their 'lumen' being

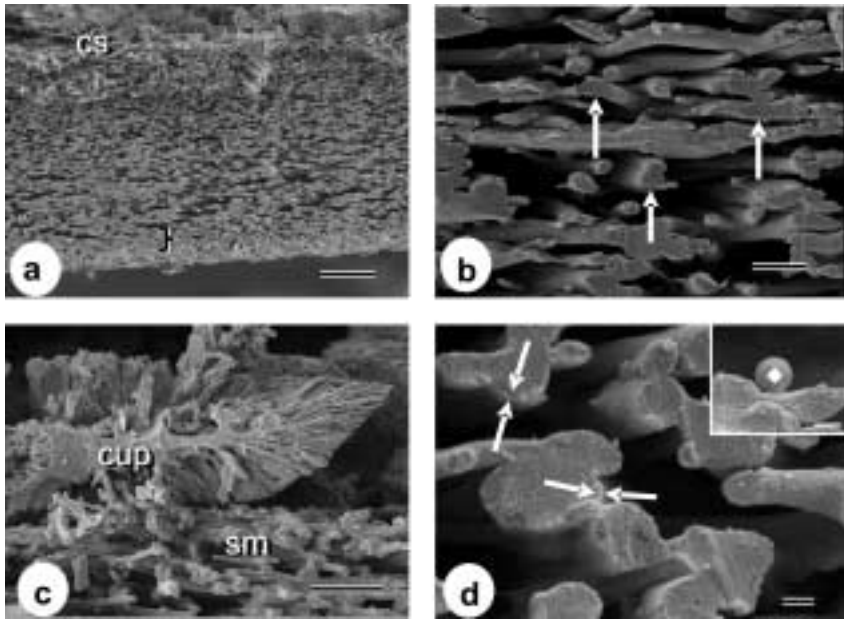

Fig. 4: **Scanning electron micrographs of the shell membrane;** a: **cross-section through the dry membrane – note the increased compaction of fibres** (bracket) **at the edge opposite the calcification surface** (cs)**;** b: **a higher magnification of the individual fibres in the membrane – arrows point to where 2 or more fibres have fused;** c: **calcification surface with part of a cup-shaped structure** (cup) **on the outer surface of the shell membrane** (sm)**;** d: **higher magnification of the fibres in a fixed membrane – a distinct separate outer layer is discernible** (between arrows) **surrounding the 'core', inset shows a bacterial particle** (◆) **attached to the fibre's surface.** (Scale bars: a, 50 µm; b, 5 µm; c, 10 µm; d, 0.5 µm.)

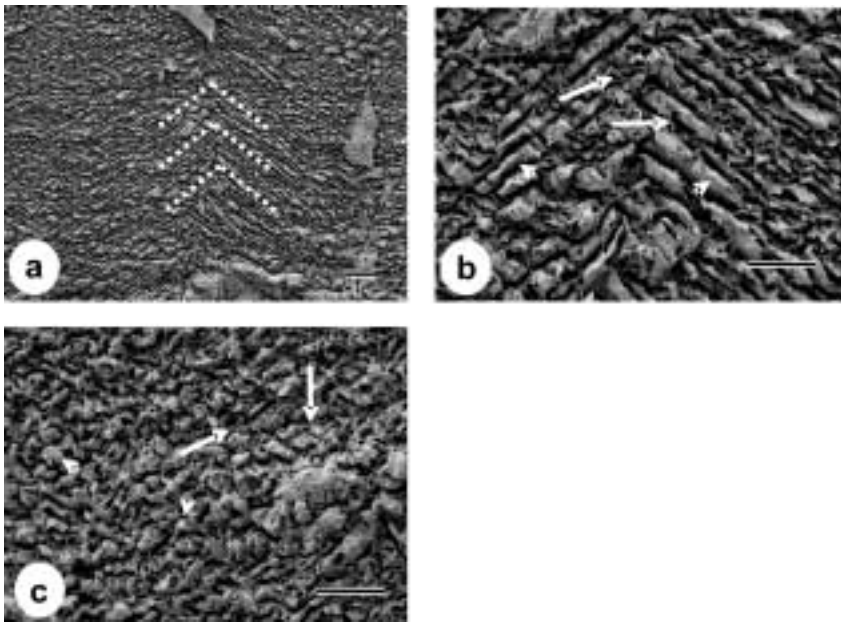

Fig. 5: **Scanning electron micrographs of deep-etched ostrich eggshell;** a: **the herringbone structure of the mammillary layer is clearly distinguishable** (broken lines)**;** b: **a higher magnification of the crystallites in the mammillary layer** (arrowheads) **with the presence of fine fibrillar material** (arrows)**;** c: **the more randomly orientated crystallite morphology of the palisade layer** (arrowheads) **with an increased presence of fibrillar material** (arrows). (Scale bars: a, 20 µm; b, 10 µm; c, 10 µm.)

devoid of material (Fig. 6c,d).

Fully decalcified sections of the eggshell had the appearance of a fibrous mat with a variable mesh. A different mesh diameter was observed in each layer of the decalcified section examined, thus the mammillary layer and lowest portions of the palisade layer had an open mesh (Fig. 7a), which decreased in size as the VCL was approached (Fig. 7b–d). The fibres making up the mesh were approximately 2.7 µm in diameter and in the mammillary and palisade layers bacteria were observed attached to the fibres of the mesh. There was a sharp delineation 8 µm from the surface of the shell. At this point the mesh solidified into an amorphous mass with no structural features that were discernible using standard SEM viewing parameters (Fig. 8a). Large openings were observed throughout the decalcified section. These openings had smoother amorphous sides that were similar in appearance to the amorphous mass of the upper 8 µm of the decalcified shell (Fig. 8b).

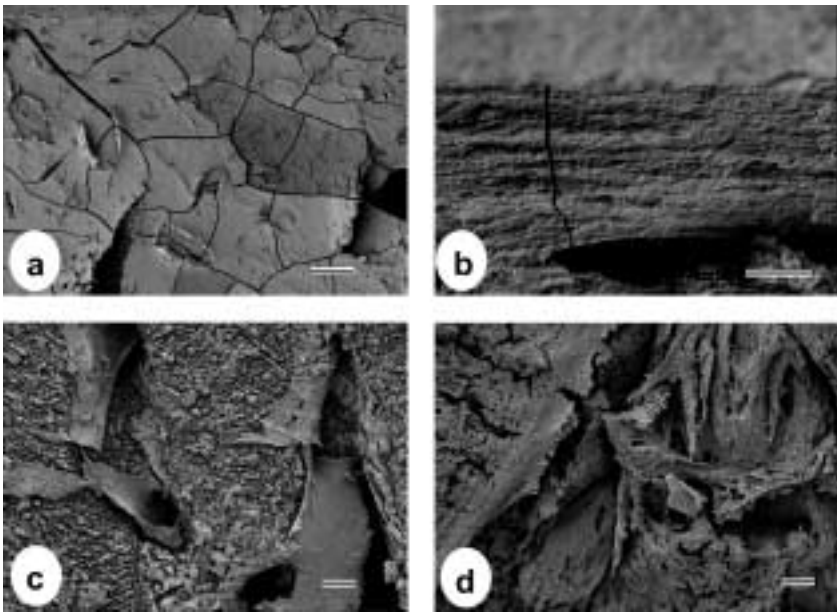

Fig. 6: **Scanning electron micrographs of a deep-etched ostrich eggshell;** a & b: **the gelatinous layer observed following deep-etching – (a) the outer surface is similar to a calcified shell while (b) the cross-section appears featureless;** c: **fibrous material running into holes in the shell structure** (palisade layer)**;** d: **a higher magnification of an opening similar to those seen in (c) but observed in the mammillary layer.** (Scale bars: a, 250 µm; b,10 µm; c, 20 µm; d, 10 µm.)

EDS analysis

Shell membrane

Analysis of the shell membrane showed that calcium and sulphur content varied in an inverse relationship across the membrane (Fig. 9a). On the side of the CAM the sulphur content was higher than the calcium content (49:18 % respectively), while on the side of the SM/mammillary layer interface the sulphur: calcium ratio was 7.5:83 %. This change in element weight percentage, from side to side, varied significantly for both elements ($P < 0.001$). The potassium content mirrored the sulphur content of the membrane but at a lower weight percentage, ranging between 2.46 % near the CAM and 0.59 % towards the SM/mammillary layer interface. The membrane's chlorine content profile was similar to both that of sulphur and potassium but demonstrated a more linear drop in weight percentage towards the SM/mammillary layer interface, from a high of 14 % to a low of 2 % (Fig. 9a). Sodium and phosphorus content remained stable, with a mean element percentages of 3.07 % and 0.52 % respectively.

Matrix

Significant differences existed in the elemental composition of the gelatinous material and in the 2 areas (A and B) examined in the deep-etched shell that retained the gelatinous material (Table 4). The gelatinous material and area A carbon content, as compared with area B, were significantly different ($P < 0.001$), with the carbon content of area B, in the deep-etched sample, being almost 3 times less than in the other 2 analyses. The sulphur content was significantly different in the gelatinous material compared to either area A or B ($P < 0.001$), decreasing significantly as the area that was probed extended deeper into the deep-etched specimen (Fig. 9b). The minor element magnesium was absent from the gelatinous material but was found in increasing quantities with increasing depth of probing in the deep-etched specimen (Fig. 9b).

DISCUSSION

Shell membrane

The avian eggshell membrane is normally divided into 2 distinct layers, a designation that is based on the weave and diameter of the fibres present[2]. In the present study, the morphological evi-

Table 4: **Mean percentage weight and standard deviation (SD) of the elements carbon, calcium, magnesium and sulphur derived from the EDS analysis of the gelatinous material (gel) and area A and B in the deep-etched samples.**

Element:	Carbon			Calcium[#]			Magnesium			Sulphur		
Area:	Gel*	A*	B	Gel	A	B	Gel*	A**	B	Gel*	A**	B
Mean	61.43	64.47	23.78	1.32	3.48	31.60	0.00	0.09	0.34	1.87	0.92	0.09
SD	2.84	2.28	0.46	0.71	1.24	1.31	0.00	0.02	0.06	0.55	0.06	0.02

*Significantly different from the area B ($P < 0.001$).
**Significantly different from the gel and area B ($P < 0.001$).
[#]Calcium levels are dependent on the amount of calcium removed by the etching process.

dence from the light microscope suggests the presence of 3 distinct layers in the ostrich eggshell rather than the traditional 2 observed in the chicken eggshell[2], and as has previously been reported for the ostrich[35]. However, the characteristics of the histochemical and lectin staining pattern suggest that there is only 1 shell membrane. This suggestion is supported by the SEM and TEM investigations, which indicate that there is no difference in the weave or the fibre thickness throughout the ostrich eggshell's membrane structure. Furthermore, the wide variation in fibre thickness observed using LM is probably due to the fibres' tendency to merge, as seen using SEM. As both the CAM and the cups at the SM/mammillary layer interface, as has previously been described[29], were present in the SEM and TEM samples, it is likely that the full thickness of the SM was being examined. It is thus probable that the 3 layers observed in the light microscopic study of the membrane are the result of the mechanical disruption of the membrane and movement of the fibres during LM processing. If this is the case, then the 3 layers would be the result of a processing artefact. The mechanical disruption of the membrane would also account for the discrepancy in the measurement of the membrane widths between the LM and SEM measurement, as the membrane would have been artificially widened during LM processing. Although 2 layers have previously been reported for the ostrich shell membrane[35], such an observation could be a result of 1 of 2 factors. First, an artifactual disruption of the membrane during sample preparation, fracturing of the eggshell to produce the radial section examined. Second, the small region of increased compaction may have been interpreted as denoting a distinct layer, which from the close examination of the membrane using TEM and SEM in this study appears to be a false conclusion.

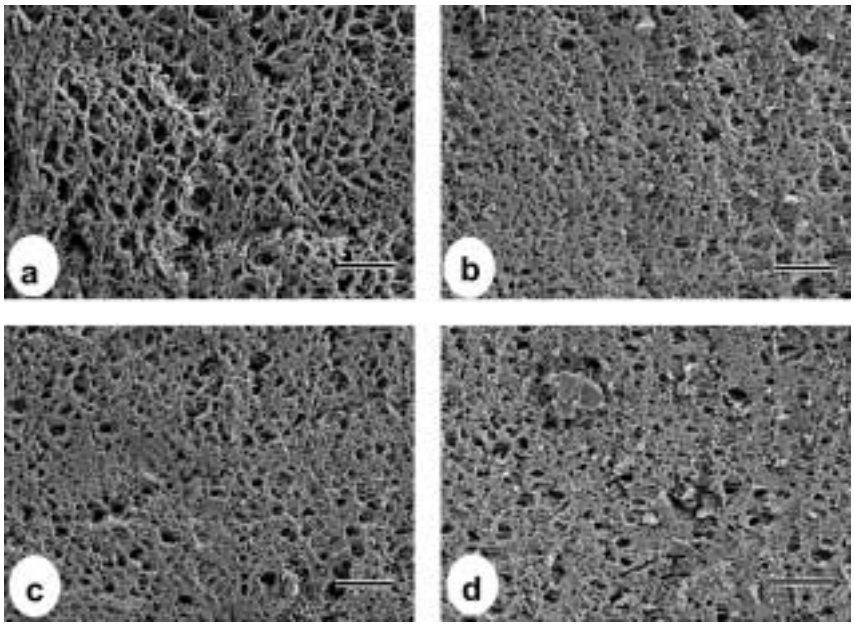

Fig. 7: **Scanning electron micrographs of a fully decalcified section of ostrich eggshell;** a: **mammillary layer;** b: **lower palisade;** c: **mid palisade;** d: **upper palisade – note the more open mesh in the deeper layers.** (Scale bars = 5 µm.)

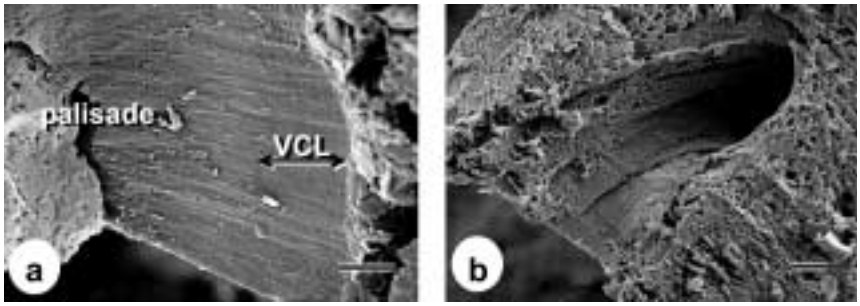

Fig. 8: **Scanning electron micrographs of a fully decalcified section of ostrich eggshell;** a: **outer area of shell corresponding to the vertical crystal layer** (VCL) **which reveals increased compaction of the mesh compared with the palisade and mammillary layers;** b: **opening of a channel lined with compacted fibres.** (Scale bars: a, 5 µm; b, 10 µm.)

The results of the limited histochemistry (the periodic acid Schiff, high-iron diamine and alcian blue staining) and immunocytochemistry suggest the presence of sulphated sialo mucins, which are probably associated with the presence of collagen, most specifically type I[33]. These findings are consistent with the report that type I collagen is the main collagenous component of the OSM of the domestic hen[2]. Although no specific staining has been undertaken regarding the collagen residues, it is possible that the same collagen central core that occurs in the fibres of the OSM of the domestic hen is present in the ostrich shell membrane. The red staining of the Masson's trichrome is indicative of non-collagenous protein, rather than the collagen that the other stains indicate. Therefore, it is likely to be staining components of the muccopolysaccharide mantle, which may be more accessible and thus mask any collagen residue staining when using this staining technique.

The TEM morphology of the fibres that compose the ostrich's shell membrane is similar to descriptions of the OSM from the domestic hen[2]. In both instances an outer mantle encapsulates the inner core of the fibre, a finding confirmed when

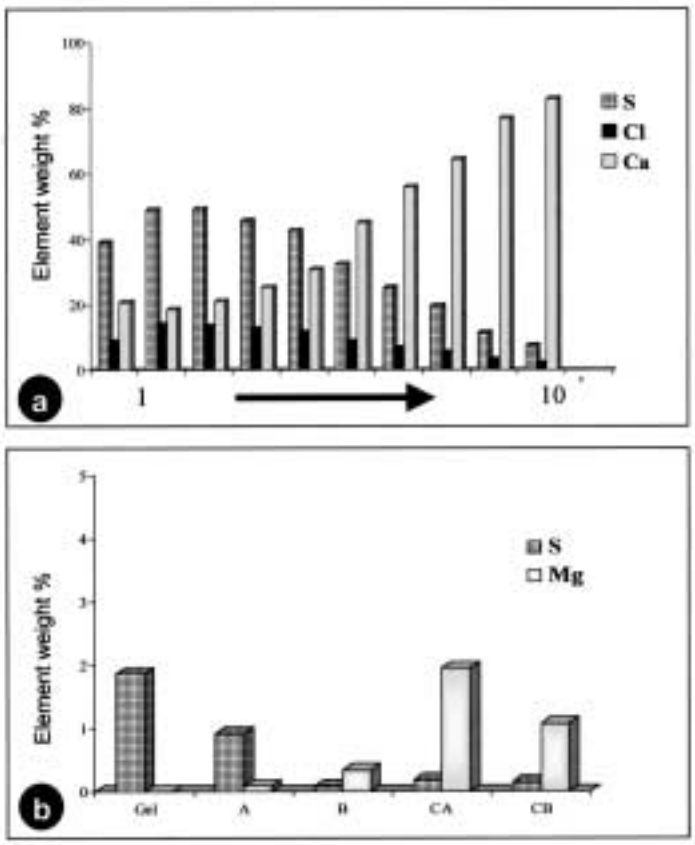

Fig. 9: **Graph representing the EDS analysis of** (a) **shell membrane and** (b) **the regions of the matrix similar to those sampled by Richards *et al.*[29]. In (a) note the inverse relationship between the sulphur and calcium content across the membrane** (1 = CAM; 10 = calcification surface). **In (b) the percentage weight of sulphur and magnesium present in the gelatinous material** (gel) **is compared to that in areas A and B in the deep-etched samples and the same areas in the calcified sample** (CA and CB). **Note the increase in sulphur in the gel, and area A compared to area B.**

examining the fixed shell membrane material with the SEM. The discrepancies observed between the measurements of the individual fibres, obtained when the dried material was observed by SEM and the fixed material by SEM and TEM, is likely to be due to the shrinkage of the mantle as it dried. From the evidence presented here it is thus unlikely that there are 2 shell membranes in the ostrich, and any division by researchers into an outer and inner shell membrane would be artificial.

Previous studies have reported the presence of a limiting membrane between the inner shell membrane and the CAM in the eggshell of the domestic hen[6] and ostrich[35]. In this study, the presence of a limiting membrane in the ostrich eggshell was confirmed, and although it is not detectable by SEM, it is quite distinct in TEM preparations. The limiting membrane in the ostrich appears to be composed of a similar material to that of the core of the fibres, rather than that of the mantle, as has been suggested for the chicken[6]. It is also apparent in the ostrich that this membrane is not continuous, as it is in the chicken, thus indicating that the composition of the limiting membrane may necessitate this discontinuous-type structure. It is feasible that the core protein is not as amenable to gaseous and ionic exchange as the mucopolysaccharides of the mantle, necessitating the existence of pores in the limiting membrane of the ostrich shell membrane. Such an arrangement would make the embryonic compartment extremely vulnerable to infection during development, unless an effective barrier was present.

In the domestic hen the shell membranes are not impervious to microorganism penetration[16]. However, evidence from the TEM and SEM study of these membranes, in the ostrich, suggests that the fibres of the membrane act as an effective barrier against microbial penetration. The increase in numbers of bacteria near the lower portions of the membrane's matrix, and the continuity of the bacterial cell wall with the structure of the fibre, suggest that bacteria are effectively trapped by an interaction between the outer mantle and the bacterial cell wall. This interaction may be similar to that of bacterial particles with the mucopolysacharrides of the mammalian inner ear[7] or reproductive tract[13]. However, considering that it is the reproductive organs of the ostrich that produce the egg, there is a high probability that the protective mechanism is similar to the barrier properties of the Muc 1-containing glycoconjugates of the mammalian reproductive tract[13]. Such an effective barrier would prevent penetration of bacteria through the discontinuous limiting membrane into the embryonic chamber.

The biochemical composition of the shell membrane appears to change at the calcification surface. The histochemical evidence suggests that the mucopolysaccharides at the surface and those associated with the cup-shaped structures are strongly sulphated enzyme-resistant sialomucins[5] that are high in galactose residues[28]. However, the EDS analysis of the membrane suggests that the sulphur is located more towards the CAM than at the calcification surface. The EDS results obtained for the membrane near the calcification surface in this study are in accord with those previously reported for the cups and fibres[29]. This apparent inconsistency between the EDS and histochemical findings may be explained if the specimen was tilted in such a manner that the spectra obtained emanated from the calcification surface (Fig. 1b). It can then be suggested that the membrane below the cups and calcification surface are high in sulphur, agreeing with the histochemical results, while the calcification surface and the cups are calcium-rich and sulphur-poor, in agreement with previous findings for this surface[29].

The Masson's trichrome stained the calcification surface a blue-green, which is indicative of collagen, and thus is in agreement with the strong lectin staining of this surface. However, as there is no mantle associated with the cup structures, the morphological localisation of the mucopolysaccharide residues stained with the alcian blue is not clear. It may be that they form an 'amorphous ground substance', such as is formed in the extracellular matrix of mammals[34], which is not as structured as the mantle. A previous study has suggested that the cup-shaped structures of the shell membrane are the sites for the initial calcification events[29]. They further suggest that these cups may be composed of type X collagen, which is known to be associated with calcification processes in the chicken[3,32]. The results of the present study tend to support the hypothesis of this previous study[29] with the evidence for a strong collagen presence in this layer.

Matrix

The ostrich shell matrix, like that of the hen, is devoid of nuclei. The blue/green colouration of the matrix with Masson's

trichrome stain is indicative of collagen or osteoid, the unmineralised bone matrix[5], while the histochemical profile of the shell matrix appears to indicate a mucopolysaccharide composition similar to the major component of the shell membrane. However, the negative reaction to the PAS stain seems to indicate that the composition of the matrix is an enzyme-resistant sialomucin[5] similar to that found at the calcification surface. The gradient in sulphated residues, as determined by the alcian blue staining and EDS analysis, from low sulphation in the deeper layers to high sulphation in the upper layers, is in accordance with the distribution of chondroitin and dermatan sulphates in the matrix of the domestic hen[11]. Another study has also immunocytochemically detected keratin sulphate[1] for the same region of the domestic hen's egg. It is likely therefore that the matrix biology of the ostrich shell is similar to that of other avian species but with variations reflecting taxonomic differences[24]. If this is the case then the core proteins of the mucopolysaccharides of the matrix are unlikely to be collagen but are rather osteopontin, ovocleidin and ovalbumin[17,24]. As osteopontin is present in osteoid tissue[21], the blue/green staining of the matrix with Masson's trichrome may reflect the presence of this protein.

Closer packing of the fine fibrillar network, as seen with the TEM, mirrors the change in the structure towards the outermost region of the matrix that is seen in the SEM images of the VCL layer. Furthermore, the increased carbon signals, using the EDS in this region (region A), appear to confirm this finding. The decreased carbon content in area B would increase the amount of space for calcium crystallite formation. However, the increased calcium and magnesium content in this area is probably not a reflection of this hypothesis but more a reflection of the efficiency of the etching process used. It is probable therefore that the gelatinous material obtained from the deep-etched shell following 48 days in the etching/de-calcifying solution corresponds to this area of changed structure. The change in structure has 2 possible explanations. First, it may represent the remains of an organic ancillary layer, which over time has become calcified as suggested in earlier work[29]. This hypothesis is supported by the increased galactose residues, as demonstrated by the lectin staining in this and preliminary work[28] and is consistent with the composition of the organic cuticle of the domestic hen[2]. However, the second suggestion, which is more likely, is that it reflects a morphologically discernible termination signal for the calcification process. As discussed above, the LM alcian blue staining pattern suggests an increase in sulphation of the glycoproteins in this region (confirmed by the EDS results), which is histochemically similar to the calcification layer, particularly the cup-shaped structures that are thought to contain proteins that inhibit calcification, particularly type X collagen[29]. However, as pointed out above, osteopontin or ovocleidin are more likely to be the protein(s) involved in matrix formation, the former being associated with the inhibition of calcification in other biomineralised tissues[21]. Thus, an increase in any of these proteins may be a means of limiting the calcification process. A biochemical change that increases the prominence of one protein over another will automatically change the morphological appearance of a region, as is seen in the present study. Changes to the organic matrix at this point will also determine the crystalline structure of the region, which possibly explains why the VCL is greatly different from the rest of the shell[29]. A number of the osteoid proteins (osteopontin and bone sialoproteins), and probably the avian counterparts (ovocleidin and ovocalcin), control size and speed of crystallite formation[30]. Thus, a change of matrix protein may also signal a change to the crystallite growth pattern.

The columnar structures that stained at the low alcian blue pH in the palisade layer probably reflect the presence of the shell pores. The channels/tubes observed in both the deep-etched and fully decalcified specimens also appear to represent shell pores. The particular histochemical staining of these structures and their similar structural appearance to the VCL region, as observed by TEM, suggests that the fibrous lining of the pores may be explained by the 2 hypotheses suggested for the matrix in the VCL region. If, as has been suggested above, the VCL is a calcified ancillary layer, then the lining of the pores is possibly capable of defence against bacterial invasion of the embryonic chamber. The sulphated sialyl mucins have been shown to play a protective role in mammalian systems, interacting with the pili on bacterial surfaces, and may thus perform a similar function in the pore walls[23,31]. The structural signal for the termination of calcification may also be relevant as a determinant of pore structure. The denser matrix would also lead to increased stability of the pore channel than would the looser matrix seen in the body of the shell.

A previous study observed a repeat pattern of the small pores in the palisade layer[29], but such a pattern could not be associated with any structure observed in the SEM images of the decalcified material. However, if the hypothesis regarding the waves of calcium-rich fluid proposed in the previous study[29] is correct, then entrapment of air bubbles in the organic matrix could explain the presence of these pores. The more compact region observed in the VCL, however, is incompatible with such bubble formation and entrapment, and would lead to the absence of pores in this area[29]. The tubular structures with increased mesh observed in the TEM images occur regularly, although no pattern is discernible. These tubular structures have an inner dimension consistent with the pore size previously reported[29]. However, if an increased mesh is indicative of a termination signal, as may be concluded from the discussion above regarding the VCL, then these areas could represent non-calcified tubes, which would show up as pores in etched sections. The purpose of such structures is unclear and may simply reflect a form of reinforcement of the shell in a similar fashion to the rods of reinforced concrete.

The herringbone structure observed in the mammillary layer of the deep-etched samples confirms the earlier findings of a dendritic-type crystallisation process in this region[29]. The more haphazard structures of the palisade layer also appear to confirm the possible growth characteristics, namely a slower crystallite growth, for this region[29].

The results of this study suggest a number of possible explanations for the increased intra-shell embryonic deaths of ostriches that have been reported[10,18]. If the lining of the pore is a part of the defence mechanism of the ostrich's egg, then the act of dipping may compromise the integrity of these structures. For example, if the eggs are warmer than the solution being used to dip the eggs, the dipping solution may penetrate the egg through the pores as a result of differential temperature suction. Such suction would be created by a decrease in the internal pressure of the egg, drawing the dipping solution through the pores and so causing damage to the pore lining[15]. It has also been suggested that the post-laying period, and the temperature of the dipping solution, are important factors to consider when immersing an egg in a solution, especially with regard to the possible transportation of bacteria to the SM[15]. Such an influx of bacteria at the level of the SM would increase the chance of bacterial invasion through the discontinuities in the limiting membrane, despite the greater antibacterial properties of the

shell membrane in this species. It is unknown whether capillary action would have any effect on drawing the dipping solution into the interior of an intact egg. Considering the thickness of the ostrich eggshell, a more 'forceful' method of entry, as described above, is more likely to explain increased bacterial invasion.

Further investigation is required to ascertain the physiological purpose of the structures observed in the matrix. Should the VCL area of the matrix be acting as an ancillary layer, which is unlikely if calcification has interfered with the chemical properties of this layer, then any form of washing or dipping may render the defensive mechanism inoperable by damaging the chemical composition of the mucopolysaccharides. The higher compactness of the VCL region and the increased mucopolysaccharides in this region may also explain the surface sheen often seen in these eggshells. The cracked microscopical appearance of the surface of the ostrich egg is most likely due to the rapid drying of this layer upon laying, as a result of the high organic component. Such an area on the outer surface of the shell also affords the egg its mechanical protection, as the higher compaction acts as an energy-absorbing barrier.

In light of the foregoing results and hypotheses, the handling of ostrich eggs on commercial farms may need to be re-examined, following more comprehensive studies on these structures, to decrease the number of intra-shell embryonic deaths[18] and thus improve the economic viability of ostrich production.

ACKNOWLEDGEMENTS

We acknowledge the help of Professor John Soley from the Department of Anatomy, Faculty of Veterinary Science, University of Pretoria, Onderstepoort, who supplied the shells used in this study.

REFERENCES

1. Arias J L, Carrino D A, Fernández M S, Rodríguez J P, Dennis J E, Caplan A I 1992 Partial biochemical and immunochemical characterization of avian eggshell extracellular matrices. *Archives of Biochemistry and Biophysics* 298: 293–302
2. Arias J L, Fink D J, Xiao S-Q, Heuer A H, Caplan A I 1993 Biomineralization and eggshells: cell-mediated acellular compartments of mineralized extracellular matrix. *International Review of Cytology* 145: 217–250
3. Arias J L, Nakamura O, Fernández M S, Wu J-J, Knigge P, Eyre D R, Caplan A I 1997 Role of type X collagen on experimental mineralization of eggshell membranes *Connective Tissue Research* 36: 21–33
4. Baker J R, Balch D A 1962 A study of the organic material of hen's-egg shell. *Biochemical Journal* 82: 352–361
5. Bancroft J D, Stevens A 1982 *Theory and practice of histological techniques* (2nd edn) Churchill Livingstone, London
6. Bellairs R, Boyde A 1969 Scanning electron microscopy of the shell membranes of the hen's egg. *Zeitschrift für Zellforschung und Mikroskopische Anatomie* 96: 237–249
7. Bernstein J M, Reddy M 2000 Bacteria-mucin interaction in the upper aerodigestive tract shows striking heterogeneity: implications in otitis media, rhinosinusitis and pneumonia. *Otolaryngology – Head & Neck Surgery* 122: 514–520
8. Board R G, Scott V D 1980 Porosity of the avian eggshell. *American Zoology* 20: 339–349
9. Board R G, Tullett S G, Perrott H R 1977 An arbitrary classification of the pore systems in avian eggshells. *Journal of Zoology, London* 182: 251–265
10. Brown C R, Peinke D, Loveridge A 1996 Mortality in near-term ostrich embryos during artificial incubation. *British Poultry Science* 37: 73–85
11. Carrino D A, Rodríguez J P, Caplan A I 1997 Dermatan sulfate proteoglycans from the mineralized matrix of the avian eggshell. *Connective Tissue Research* 36:175–193
12. Coetzee H L Erasmus C 1999 A lectocytochemical characterization and distribution of the glycoproteins of the gastrointestinal tract of the freshwater bream (*Oreochromis mossambicus*). *Proceedings of the Microscopy Society of Southern Africa* 29: 69
13. DeSouza M M, Surveyor G A, Price R E, Julian J, Kardon R, Zhou X, Gendler S, Hilkens J, Carson D D 1999 MUC 1/episialin: a critical barrier in the female reproductive tract. *Journal of Reproductive Immunology* 45: 127–158
14. Garcia-Ruiz M 1985 On the formation of induced morphology crystal aggregates. *Journal of Crystal Growth* 73: 251–262
15. Haines B, Moran T 1940 Porosity of, and bacterial invasion through, the shell of the hen's egg. *Journal of Hygiene* 40: 453–561
16. Haigh T, Betts W B 1991 Microbial barrier properties of hen egg shells. *Microbios* 68: 137–146
17. Hincke M T, Gautron J, Tsang C P, McKee M D, Nys Y 1999 Molecular cloning and ultrastructural localization of the core protein of an eggshell matrix proteoglycan, ovcleidin-116. *Journal of Biological Chemistry* 274: 32915–32923
18. Huchzermeyer F W 1996 High mortality in ostrich eggs and hatchlings due to egg-washing. *Journal of the South African Veterinary Association* 67: 3
19. King K 1978 Distribution of γ-carboxyglutamic acid in calcified tissues. *Biochimica et Biophysica Acta* 542: 542–546
20. Klos H-G, Langner H J, Boenigj G, Wandelburg K, Pohl H, Grund S, Eichberg J, Steglich W 1976 Chemische und pysikalische Untersuchungen an Eierschalen von vier Laufvogelarten (Struthioniformes). *Zentralblatt für Veterinarmedizin Reihe A.* 23: 413–428
21. McKee M D, Nanci A 1996 Osteopontin at mineralized tissue interfaces in bone, teeth, and osseointegrated implants: Ultrastructural distribution and implications for mineralized tissue formation, turnover, and repair. *Microscopy Research and Technique* 33:141–164
22. Nascimento V P, Cranstoun S, Solomon S E 1992 Relationship between shell structure and movement of *Salmonella enteritidis across the eggshell wall. British Poultry Science* 33: 37–48
23. Nieuw Amerongen A V, Bolscher J G, Bloemena E, Veerman E C 1998 Sulfomucins in the human body. *Biological Chemistry* 379: 1–18
24. Panheleux M, Bain M, Fernandez M S, Morales I, Gautron J, Arias J L, Solomon S E, Hincke M, Nys Y 1999 Organic matrix composition and ultrastructure of eggshell: a comparative study. *British Poultry Science* 40: 240–252
25. Peebles E D, Brake J, Gildersleeve R P 1987 Effects of eggshell cuticle removal and incubation humidity on embryonic development and hatchability of broilers. *Poultry Science* 66: 834–840
26. Richards P D G 1998 Adenylate cyclase in normal and leiomyomatous uteri. M.Sc. thesis, University of the Witwatersrand
27. Richards P D G, Botha A, Richards P A 1998 Vertical crystal layer of ostrich eggshell: one or two layers? *Proceedings of the Microscopy Society of Southern Africa* 28: 99
28. Richards P D G, Erasmus C, Richards P A 2000 Initial histochemical observations of ostrich shell organic components. *Proceedings of the Microscopy Society of Southern Africa* 30: 65
29. Richards P D G, Richards P A, Lee M E 2000 Ultrastructural characteristics of ostrich eggshell: outer shell membrane and calcified layers. *Journal of the South African Veterinary Association* 71: 97–102
30. Roach H I 1994 Why does bone matrix contain non-collagenous proteins? The possible roles of osteocalcin, osteonectin, osteopontin and bone sialoprotein in bone mineralisation and resorption. *Cell Biology International* 18: 617–628
31. Scharfman A, Degroote S, Beau J, Lamblin G, Roussel P, Mazurier J 1999 *Pseudomonas aeruginosa* binds to neoglycoconjugates bearing mucin carbohydrate determinants and predominantly to sialyl-Lewis x conjugates. *Glycobiology* 9: 757–764
32. Schmid T M, Popp R G, Linsenmayer T F 1990 Hypertrophic cartilage matrix. Type X collagen, supramolecular assembly and calcification. *Annals of the New York Academy of Sciences* 580: 64–73
33. Scott J E 1991 Proteoglycan:collagen interactions in connective tissues. Ultrastructural, biochemical, functional and evolutionary aspects. *International Journal of Biological Macromolecules* 13: 157–161
34. Scott J E 1995 Extracellular matrix, supramolecular organisation and shape. *Journal of Anatomy* 187: 259–269
35. Sparks N H C, Deeming D C 1996 Ostrich eggshell ultrastructure – a study using electron microscopy and X-ray diffraction. In Deeming D C (ed.) *Improving our understanding of ratites in a farming environment.* Manchester, UK 164–165
36. Tan C K, Chen T W, Chan H L, Ng L S 1992 A scanning and transmission electron microscopic study of the membranes of chicken egg. *Histology and Histopathology* 7: 339–345
37. Tullett S G, Board R G, Love G, Perrott H R, Scott V D 1976 Vaterite deposition during eggshell formation in the cormorant, gannet and shag, and in 'shell-less' eggs of the domestic fowl. *Acta Zoologica (Stockholm)* 57: 79–87
38. Tyler C, Simkiss K 1959 A study of the egg shells of ratite birds. *Proceedings of the Zoological Society, London* 133: 201–243